ELSEVIER

Thermochimica Acta 323 (1998) 27–36

thermochimica acta

Kinetic and thermodynamic studies of the non-isothermal decompositions of nickel malonate dihydrate and nickel hydrogen malonate dihydrate

Mohamed A. Mohamed[a,*], Andrew K. Galwey[b], Samih A. Halawy[c]

[a] *Chemistry Department, Faculty of Science, South Valley University, Qena 83511, Egypt*
[b] *Chemistry Department, Queen's University of Belfast, Belfast BT9 5AG, Ireland*
[c] *Chemistry Department, College of Education, King Faisal University, P.O. Box 1759, Hofuf 31982, Saudi Arabia*

Received 7 January 1998; received in revised form 8 June 1998; accepted 30 June 1998

Abstract

Non-isothermal decompositions (including TG, DTG, DTA and DSC) of nickel malonate dihydrate and of nickel hydrogen malonate dihydrate were studied in different dynamic atmospheres of N_2, H_2 or air. The reaction of the hydrogen malonate salt commences at a lower temperature than the corresponding nickel malonate salt.

IR spectroscopy showed that nickel acetate was formed as a reaction intermediate during the decompositions of both reactants. X-ray diffraction showed that nickel metal was the predominant product from reactions in N_2 or H_2 atmospheres while nickel oxide, together with some nickel metal, was formed during reaction in air. Gas chromatography identified CO_2, CO, acetic acid ethyl alcohol together with appreciable amounts of methyl formate and ethyl formate as the volatile decomposition products.

Kinetic and thermodynamic parameters of the decomposition of the two reactant salts were calculated. © 1998 Elsevier Science B.V. All rights reserved.

Keywords: DSC; DTA; GC; IR; Kinetics; Nickel malonate dihydrate; Nickel hydrogen malonate dihydrate; TGA; XRD

1. Introduction

Kinetic and mechanistic studies of the thermal decompositions of a number of metal malonates (specially those of transition metals) have been reported [1–7]. These studies have revealed that the course of decomposition of metal malonates is very much influenced by the constituent metal cation present. For example, copper (II) malonate was reported [1] to decompose through two different rate processes. Analytical techniques showed that a stepwise cation reduction ($Cu^{2+} \rightarrow Cu^{+} \rightarrow Cu^{0}$) took place during the decomposition process together with the formation of copper acetate as a reaction intermediate. Scanning electron microscopy (SEM) has revealed an extensive melt formation during the first decomposition step (i.e. the decomposition of Cu^{II} to the Cu^{I} salt). Some other malonates were also found to form the corresponding acetate during the course of thermal decomposition, e.g. the calcium [2], nickel [3,4] and manganese (II) malonate [5] salts. In addition to the formation of nickel acetate, nickel malonate was also reported [3,4] to yield nickel carbide, Ni_3C. Calcium malonate was found [2] to form calcium carbonate, $CaCO_3$, as a result of the partial decomposition of calcium acetate

*Corresponding author. Tel.: +20-96-211273; fax: +20-96-211272.

0040-6031/98/$ – see front matter © 1998 Elsevier Science B.V. All rights reserved.
PII: S0040-6031(98)00492-4

intermediate with no evidence of melting. Volatile products of the decompositions of metal malonates have been shown [4] to include CO_2, CO, acetone, acetic acid and smaller yields of esters.

Silver malonate, on the other hand, was found [6,7] to decompose in the solid state through a nucleation and growth mechanism with no evidence of silver acetate intermediate formation. The volatile decomposition products of silver malonate, however, were similar to those reported [8] for the decomposition of silver acetate. This has suggested the possible intervention of silver acetate as a reaction intermediate and its rapid decomposition at the reaction temperature.

The formation of metal acetate intermediates during the decompositions of these metal malonates has prompted Galwey and Mohamed to propose a mechanism based on hydrogen transfer for these metal malonates [2]. The main objective of the present study is to test the validity of that previously proposed hydrogen-transfer mechanism [2]. Therefore, the thermal decomposition of nickel malonate dihydrate and its nickel hydrogen malonate salt are investigated in order to study the effect of presence of constituent hydrogen in the reactant salt on the course of decomposition.

2. Experimental

2.1. Materials

2.1.1. Nickel malonate

A solution of 11.85 g of $NiCl_2 \cdot 6H_2O$ in 200 ml of distilled water was added to a solution of 7.4 g of disodium malonate in 200 ml distilled water with stirring. The reaction mixture was maintained at 60°C for 3 h. The precipitate formed was filtered, washed with water and ethanol. It was finally dried in an oven at 100°C for 6 h.

2.1.2. Nickel hydrogen malonate

A suspension of 4.64 g of $Ni(OH)_2$ was added slowly, with continuous stirring, to a solution of 10.41 g of malonic acid in 200 ml of distilled water at ambient temperature and was left for 12 h. The precipitate was then filtered, washed with water and ethanol and was finally dried at 100°C.

All chemicals were analytical grade materials and were used as received.

2.2. Techniques

2.2.1. Elemental analysis

The amounts of carbon and hydrogen in the two prepared reactants were measured using combustion analysis. Nickel contents were determined using the standard atomic absorption spectroscopy technique.

2.2.2. Thermal analysis

Thermal analyses experiments (including thermogravimetry, TGA, derivative thermogravimetry, DTG, differential thermal analysis, DTA, and differential scanning calorimetry, DSC) were performed using a Shimadzu 'Stand Alone' thermal analyzer (TGA-50H, DTA-50 and DSC-50), Japan. The thermal analyzer is equipped with a data acquisition and handling system (Chromatopac C-R4AD).

Experiments were carried out in a dynamic atmosphere (40 ml/min) of N_2, H_2 or air. Air was excluded from all DSC experiments to avoid the possible oxidation of the copper pans of the instrument. Equal weights (ca. 10–15 mg) of gently crushed samples were used to minimize the effect of variation in sample weight and particle size variation [9].

Highly sintered α-Al_2O_3 powder (Shimadzu) was used as a reference material for DTA and DSC experiments. Specpure Indium metal, Johnson Matthey, was used for calibration of the DSC instrument (melting point=157°C and ΔH=28.24 Jg^{-1} [10]).

2.2.3. IR spectroscopy

IR spectroscopy of the reactants, samples decomposed to some selected temperatures (in different atmospheres) and the residual solid products were carried out by the KBr disk technique using a Nicolet FTIR-spectrophotometer model Magna IR-560.

2.2.4. X-ray diffraction

X-ray powder diffraction analysis of the parent reactants together with their decomposition solid products was carried out using a model D5000 Siemens diffractometer (Germany), equipped with a copper anode generating Ni-filtered CuK_α radiation (λ=1.5418 Å). Data acquisition and handling system (Diffrac software, Siemens) was used for identification purposes.

2.2.5. Gas chromatography

Volatile decomposition products of both nickel salts were analysed using a Shimadzu computerized gas chromatograph model GC-14A, connected with a flow system at atmospheric pressure. Product gases were sensed by a thermal conductivity detector. Automatic sampling was performed with a heated gas sampling cock type HGS-2.

2.2.6. Data processing

Kinetic parameters, i.e. the activation energy (E_a kJ mol^{-1}) and the frequency factor (ln A) were calculated for the dehydration and decomposition processes using Ozawa equation [11]

$$\ln \phi/T_m^2 = -E_a/RT + \ln R/\theta E_a \quad (1)$$

where ϕ is the heating rate (deg min^{-1}), T_m the DTG peak maximum temperature, R the gas constant (8.314 J mol^{-1}°C^{-1}), and θ=(1/A). The kinetic parameters of the weight invariant process (i.e. the recrystallization step, *vide infra*) were calculated from the DTA data using Kissinger equation [12]:

$$\ln \phi/T_m^2 = -E_a/RT + \ln AR/E_a$$

This equation is distinct in adopting the DTA results. Thus, it is superior [13] to the other methods for its ability to handle not only the mass-variant, but also the mass-invariant processes. The disadvantage of Kissinger equation is that it does not consider the actual reaction order (n) [13].

DSC measurements were used to calculate some thermodynamic parameters (i.e. enthalpy change, ΔH, heat capacity, C_p, and the entropy change, ΔS). Details of the calculations of the kinetic and thermodynamic parameters were given elsewhere [14].

3. Results and discussion

3.1. Elemental analysis

The results of combustion analysis and atomic absorption analysis of the two reactants corresponded closely with the theoretical expectation for the dihydrate composition. Results were as follows:

For NiMal salt: 18.8% C (18.31); 3.7% H (3.07) and 30.21% Ni (29.83).

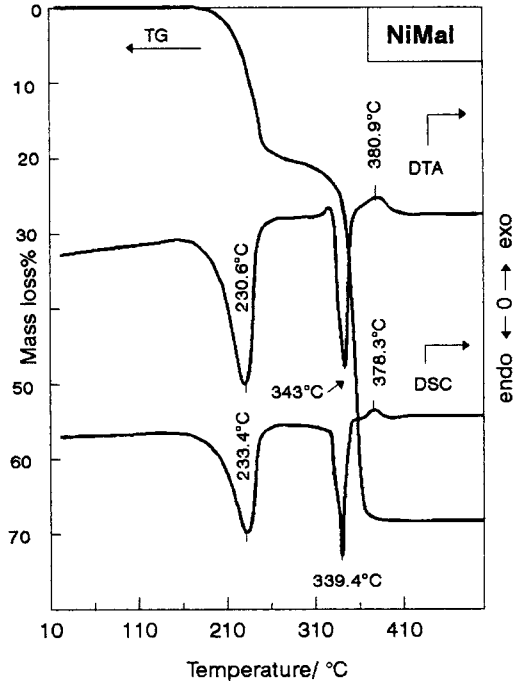

Fig. 1. TG, DTA and DSC curves of the decomposition of NiMal at a heating rate of 5°C/min under a dynamic atmosphere (40 ml/min) of N_2.

For NiHMal salt: 25.1% C (23.95); 3.8% H (3.35) and 19.81% Ni (19.51).

3.2. Thermal analyses

3.2.1. Nickel malonate dihydrate (NiMal)

Fig. 1 shows TG, DTA and DSC curves of NiMal in N_2 atmosphere. The TG curve displays two steps. The first, between 185–258°C, is accompanied by 18.6% mass loss which is attributed to the dehydration process ($-2H_2O \approx 18.3\%$). The second step, between 258–367°C, is associated with 49.6% mass loss which is attributed to the decomposition. This brings the total mass loss to 68.2% of the original mass of sample which is greater than that expected for the formation of NiO (62.0%) and is smaller than that expected for the formation of nickel metal (70.2%). Therefore, Ni metal may constitute the major component of the solid residue together with a small proportion of NiO and some carbon expected to result from the anion breakdown process [3].

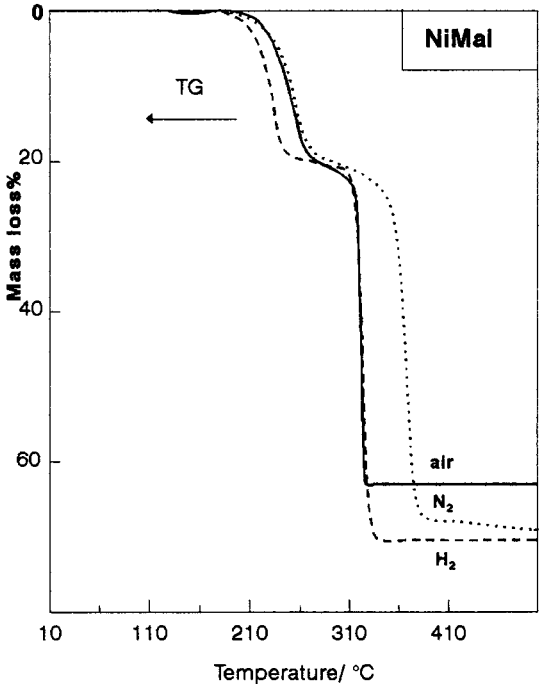

Fig. 2. Three TG curves of NiMal decomposition performed at a heating rate of 10°C/min in a dynamic atmosphere (40 ml/min) of N_2 (———), H_2 (– – –) and air (· · ·).

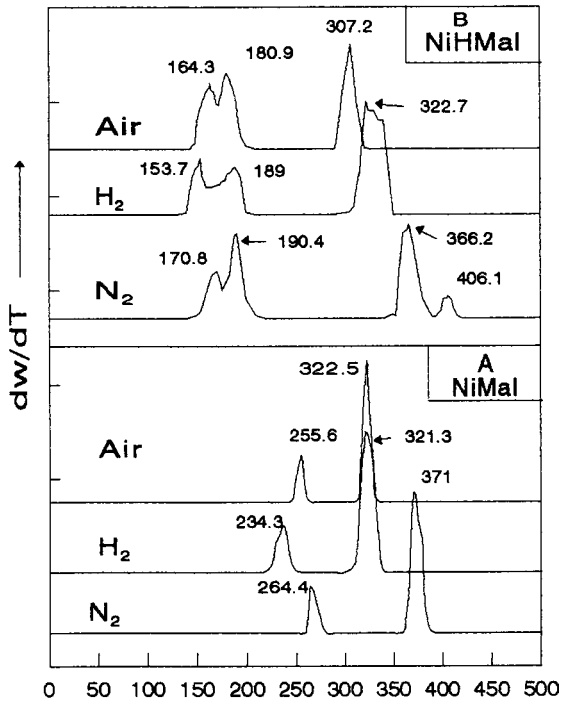

Fig. 3. DTG curves of the decomposition of (A) NiMal and (B) NiHMal at 10°C/min under different atmospheres of N_2, H_2 and air.

DTG curve at the same rate possessed two peaks of maximum rate of mass loss maximized at 245° and 359°C for the dehydration and decomposition processes.

The DTA curve shows two endothermic peaks which are attributed to the dehydration and decomposition processes. In addition, there is a weak exotherm at 380.9°C. Since there is no mass loss at that temperature, this event could be a physical process, i.e. recrystallization of a product solid. The DSC curve is very similar to the DTA curve except that the exotherm is relatively sharper.

The effect of gas atmosphere on the TG curves of NiMal is shown in Fig. 2. It is clear that the rate of reaction in H_2 (or in air) was faster than in N_2 and the decomposition was completed earlier (by ca. 50°C). The total mass loss in H_2 (ca. 70.0%) suggested the formation of Ni metal residue (70.2%). The DTG plots under different atmospheres (all at 10°C/min) are shown in Fig. 3. DTG curve in H_2 showed the two maxima at 234.3° and 321.3°C. In air, however, the measured total mass loss was 62.2%, suggesting the formation of solid residue rich in NiO. The DTG curve in air gave its two maxima at 255.6° and 322.5°C.

Fig. 4 shows the effect of H_2 on the DTA curve of NiMal. Compared with DTA in N_2, three differences were observed:

1. The dehydration and decomposition steps were shifted towards lower temperatures, a similar behaviour to that reported before for silver [7] and manganese malonates [5].
2. The decomposition process appeared as two endothermic peaks instead of one sharp endotherm observed in N_2.
3. The appearance of a sharp exothermic peak at the very end of the decomposition. This may be ascribed to the reduction of NiO present in the solid residue.

3.2.2. Nickel hydrogen malonate dihydrate (NiHMal)

Fig. 5 shows TG, DTA and DSC curves of NiHMal in N_2. The TG curve displays two main mass loss steps. The first between 122–236°C with 42.6% mass

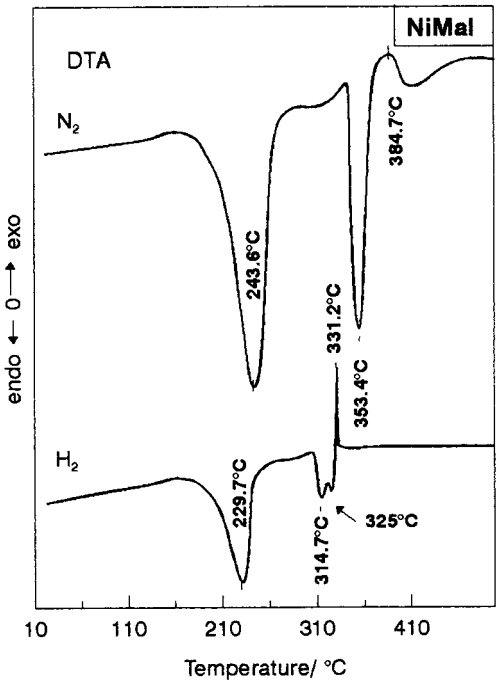

Fig. 4. Two DTA curves of NiMal decomposition carried out at a heating rate of 10°C/min, one in N_2 atmosphere and the other in H_2.

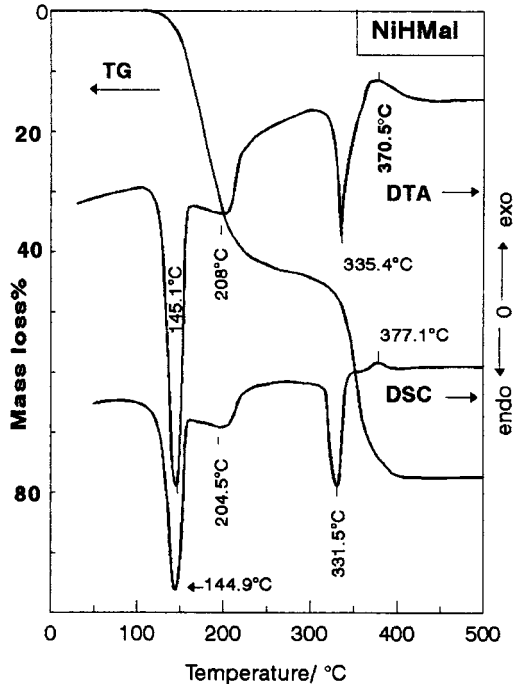

Fig. 5. TG, DTA and DSC curves of the decomposition of NiHMal at a heating rate of 5°C/min under a dynamic atmosphere (40 ml/min) of N_2.

loss (12.2% dehydration and 30.4% partial decomposition of the anhydrous salt). The second step appeared between 240–402°C (with 34.3% loss). The total mass loss was 76.9% of the original sample mass which suggests that the final solid residue composed of Ni metal with small amounts of NiO and some carbonaceous residue. The DTG curve of NiHMal possessed four peaks located at 156.9 (dehydration), 176.3 (partial decomposition), 353 and 379.8°C (decomposition).

DTA curve of NiHMal showed three endothermic peaks together with a small exothermic peak. The DSC curve is very similar to the DTA curve (see Fig. 5).

The effect of gas atmosphere (N_2, H_2 or air) on the TG curve of NiHMal is displayed in Fig. 6. It reveals that the decomposition in H_2 (or air) is faster (by ≈80–120°C) than in N_2. The number of mass loss steps (and consequently the DTG peaks) in H_2 (or air) were reduced to three steps instead of four in case of N_2 (see Fig. 3). The total mass loss in H_2 (ca. 80.4%) suggested that Ni metal is the major component of the solid product. In air, however, the mass loss (ca. 75.2%) suggested NiO to be the major solid product.

The effect of H_2 atmosphere on the DTA curve of NiHMal is shown in Fig. 7. The use of H_2 has resulted in a general shift towards lower temperatures for all peaks and, in addition, the decomposition process appeared as two endotherms instead of one broad peak in N_2, a similar behaviour to that shown for NiMal reactant (see Fig. 4). The final weak exotherm in H_2 is attributed to the reduction of the NiO to Ni metal.

It should be noted, here, that a slight mass increase was observed after the complete decomposition of both nickel salts in N_2 atmosphere. This phenomenon has been reported before [15] and was attributed to the oxidation of some of the Ni metal present in the solid residue by traces of oxygen in the N_2 gas. This phenomenon takes place as a result of the pyrophoric properties [15] of the Ni metal decomposition product.

It is concluded from Figs. 1 and 5 that NiMal is relatively more stable than NiHMal, whereas in N_2 atmosphere the decomposition of the latter salt has

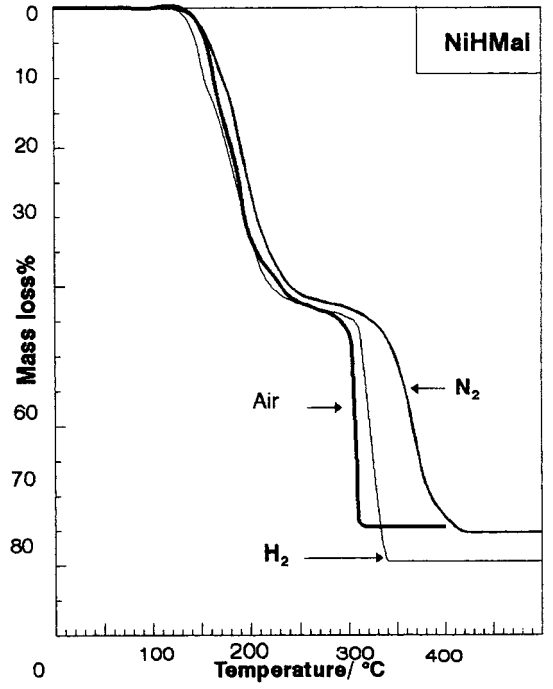

Fig. 6. Three TG curves of NiHMal decomposition performed at a heating rate of 10°C/min under a dynamic atmosphere (40 ml/min) of N_2, H_2 and air.

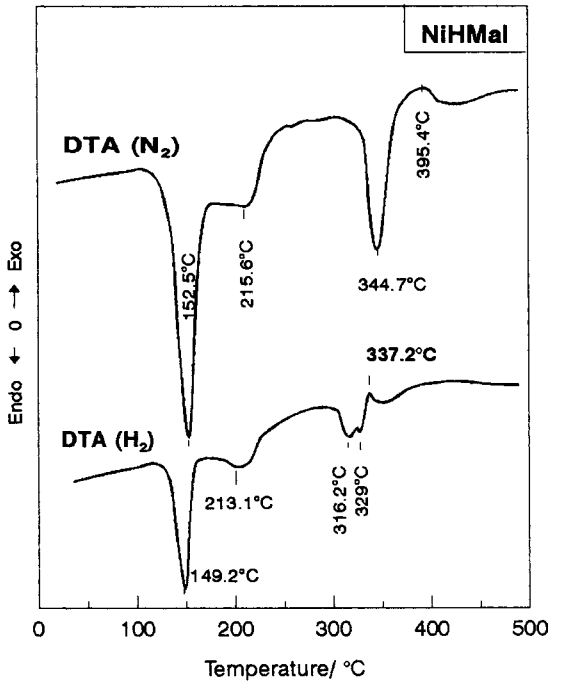

Fig. 7. Two DTA curves of NiHMal dihydrate decomposition carried out at a heating rate of 10°C/min, one in N_2 atmosphere and the other in H_2.

started ca. 70°C lower than the former. The decomposition temperature range for the final step in both salts was approximately the same which suggests a later reaction of identical species.

3.3. Kinetic and thermodynamic parameters

The kinetic and thermodynamic parameters of both reactants (for all processes) are given in Table 1. From the data in Table 1, we can conclude the following:

1. The activation energy calculated in N_2 for the decomposition of NiMal (ca. 190 kJ/mol) is reasonably close to that reported previously (ca. 176 kJ/mol) for the decomposition under vacuum [3].
2. Effect of the prevailing atmosphere on the activation energy of the decomposition of both nickel salts was in the following order: E_a(air)>E_a (H_2)>E_a(N_2), which is in accordance with a similar comparative study of some metal malonates [16].
3. E_a values calculated for the dehydration and the decomposition of NiHMal were lower than the corresponding E_a values of NiMal. This further confirms that NiMal is thermally more stable than NiHMal.
4. Values of ΔH, C_p and ΔS for the decomposition of NiMal were very close to those of the second decomposition step (decomp. 2 in Table 1) of NiHMal. This further supports the conclusion that, above 270°C, both salts behave similarly (see Table 1).

3.4. IR spectroscopy

Two important observations could summarize the IR spectra taken at different temperatures for both salts:

1. The spectra of both salts after heating to 270°C in N_2 atmosphere became almost identical. This indicates that after dehydration and partial decomposition of NiHMal (see Fig. 5), it gave an

Table 1
Kinetic and thermodynamic parameters for the decomposition of Nickel malonate dihydrate and nickel hydrogen malonate dihydrate

Parameter	Process	NiMal			NiHMal		
		N_2	H_2	Air	N_2	H_2	Air
E_a	Dehyd.	105±5	169±5	154±4	71.5±3	76.3±4	82.5±6
	Decomp. 1	—	—	—	125±4	—	—
	Decomp. 2	190±7	425±11	993±21	141±4	407±9	897±23
	Recryst. [a]	138.3±6	—	—	121.6±4	—	—
ln A	Dehyd.	26±1.7	33.6±2.1	27.9±1.9	109±0.3	7.8±0.2	1 2 . 9 - ±0.4
	Decomp. 1	—	—	—	22.8±1.1	68±3	243±11
	Decomp. 2	39±2	79±5	274±15	28.4±1.3	—	—
	Recryst. [a]	21.8±1.1	—	—	14±0.6	—	—
ΔH	Dehyd.	121.4±7	39.7±2	—	121±6	36.8±2	—
	Decomp. 1	—	—	—	29.5±1.7	11±1	—
	Decomp. 2	46.7±3	18.8±1.1	—	51.7±3	13.4±1.2	—
	Recryst.	2.2±0.1	4.16±0.3	—	2.12±0.4	—	—
C_p	Dehyd.	0.85±0.09	0.49±0.07	—	2.37±0.1	0.88±0.08	—
	Decomp. 1	—	—	—	0.48±0.08	0.13±0.02	—
	Decomp. 2	0.83±0.1	0.71±0.07	—	0.84±0.11	0.39±0.06	—
	Recryst.	0.09±0.01	0.60±0.05	—	0.07±0.01	—	—
ΔS	Dehyd.	0.21±0.02	0.08±0.01	—	0.30±0.04	0.09±0.01	—
	Decomp. 1	—	—	—	0.064±0.01	0.022±0.002	—
	Decomp. 2	0.08±0.01	0.032±0.004	—	0.088±0.011	0.23±0.03	—
	Recryst.	0.004±0.001	0.007±0.001	—	0.003±0.001	—	—

[a] Values calculated from DTA data.

identical product to that of NiMal after its dehydration (e.g. both showed peaks at 810, 730 cm^{-1} (OCO) and at 1270 cm^{-1} (CH_2)) [17].
2. Above 270°C and up to 340°C, both salts showed two new peaks at 1020 and 1050 cm^{-1} attributed to acetate anion [18]. These two peaks appeared rather earlier for NiHMal than for NiMal. Above 350°C, all peaks due to organic groupings began to diminish.

The participation of nickel acetate intermediate in the decompositions of both salts was further shown in Fig. 8. The DTA curve of the mixture of 10% (by weight) of nickel acetate with NiMal showed that the main decomposition endotherm appeared at almost the same temperature as for NiMal and nickel acetate curves. We conclude, therefore, that NiMal decomposes through the formation and subsequent decomposition of nickel acetate as a reaction intermediate.

3.5. X-ray analysis

Fig. 9 shows the XRD patterns (a) for NiMal and (b–e) its decomposition solid products under different atmospheres. The parent salt (pattern (a)) matched well with the ICDD [19] (data no. 24-1840) of the dihydrate composition confirming the elemental analysis results.

Pattern (b) (300°C in N_2) shows the characteristic d-spacings of Ni metal (ICDD no. 4-0850) and nickel carbide, Ni_3C, (ICDD no. 6-0697). This compound, Ni_3C, was reported to form during the decompositions of nickel malonate [3] and of nickel acetate [4].

Patterns of the solid products at 400°C have confirmed the TG results, whereas in N_2 pattern (c) shows

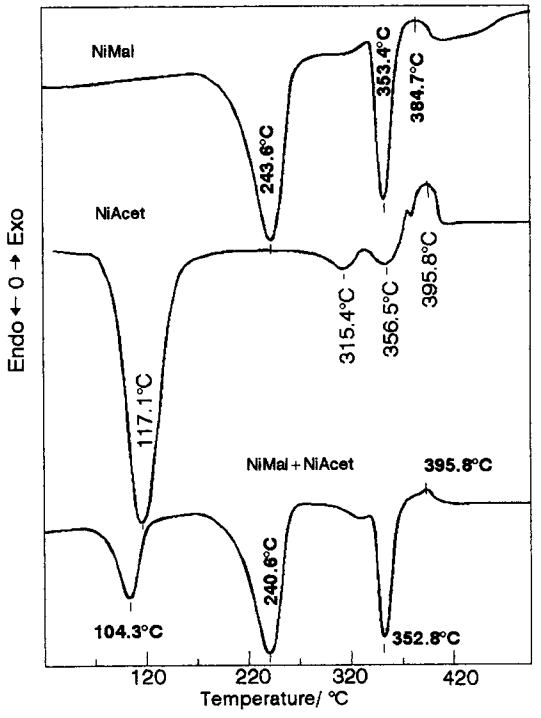

Fig. 8. Three DTA curves carried out at a heating rate of 10°C/min under a dynamic atmosphere (40 ml/min) of N_2 for pure NiMal, nickel acetate hydrate and for a mixture of 10% nickel acetate added to NiMal.

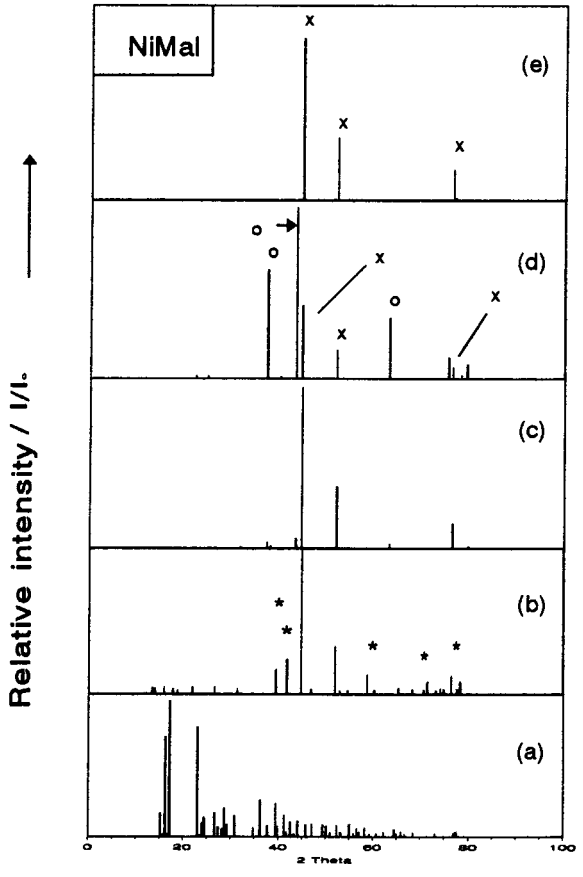

Fig. 9. XRD patterns of (a) NiMal, (b) sample decomposed to 300°C in N_2, samples decomposed to 400°C (c) in N_2, (d) in air, and (e) in H_2.

the characteristic lines of Ni metal and traces of NiO. In air (pattern (d)), NiO was the major product together with traces of Ni metal. In H_2 (pattern (d)), however, Ni metal was the only solid product (see the TG results).

Fig. 10 shows the XRD patterns of (a) NiHMal and (b–d) its solid decomposition products in different atmospheres. Pattern (a) of the parent salt confirmed that the structure of the reactant is $[C_6H_6NiO_8{\cdot}2H_2O]$ where it matched well with the ICDD data [19] (no. 26-1872 and 24-1838) for the dihydrate form (see the elemental analysis results). Patterns (b–d) of the decomposition products in N_2, air and H_2, respectively, have given similar results to those seen for NiMal (see above).

From Figs. 9 and 10, the intensity of nickel metal lines in the solid residue of NiHMal in air (Fig. 10, pattern (c)) is stronger than that of NiMal in air (Fig. 9, pattern (d)). This could be attributed to the constituent hydrogen in the NiHMal salt together with the CO gas produced.

3.6. Gas chromatography

The volatile decomposition products of NiMal and of NiHMal, after dehydration, were identified using gas chromatography as CO_2, CO, acetic acid and ethanol. The decomposition of NiHMal, however, yielded methyl formate and ethyl formate as major products below 205°C. Above 320°C, however, the volatile products were very similar to those produced from NiMal. This is further evidence that the decompositions of both salts proceed similarly, especially in the final stage.

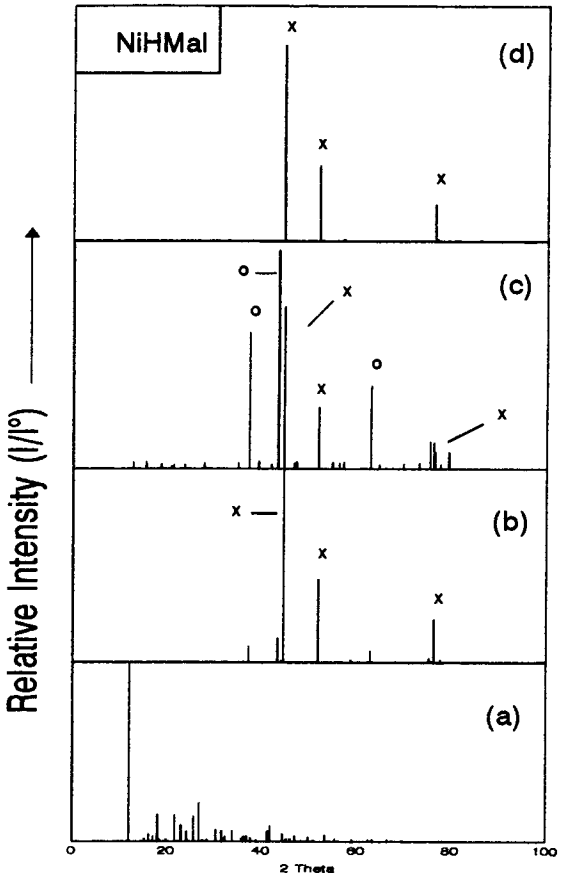

Fig. 10. XRD patterns of (a) NiHMal, (b) samples decomposed to 400°C in N_2, (c) in air, (d) and in H_2.

4. Conclusions

4.1. Dehydration reactions

4.1.1. Nickel malonate dihydrate (NiMal)

The first rate process (185–258°C in N_2, Fig. 1) was identified as reactant dehydration. The mass loss for this endothermic process is in accordance with the expectation of $-2H_2O$ in agreement with previous work [3]. Rates of this reaction in air or N_2 were similar but H_2O loss was appreciably (−14°C) more rapid in H_2. It seems unlikely that this is due to chemical reactions but may reasonably be ascribed to increased heat transfer and rapidity of diffusion of H_2O evolved. The sensitivity of kinetic behaviour of reversible dehydration to reaction conditions and most notably the availability of water vapour has been discussed by Flanagan et al. [20]. We conclude, therefore, that the rate of dehydration of NiMal is dependent on the locally prevailing water vapour pressure because the reaction is at least partially reversible. This accounts for the range of E_a values in Table 1 which are significantly different from magnitudes previously reported for the same reaction [3]. Further work, including studies under carefully controlled reaction conditions [20], is required to measure E_a for this process.

4.1.2. Nickel hydrogen malonate dihydrate (NiHMal)

The first mass loss step, corresponding to theoretical expectation for $-2H_2O$ (122–165°C in N_2, Fig. 5) overlapped with a further process identified as decomposition (165–236°C). This dehydration occurred at a lower temperature (−90°C) and was less sensitive to conditions than the reaction of NiMal. We also notice the greater constancy of the E_a values (Table 1). These results can be explained by the assumption that water loss here is irreversible in a phase that is undergoing decomposition and is well below the temperature at which the dehydration of NiMal (the decomposition product, see below) appears to be reversible. Under these conditions, we conclude that the dehydration of NiHMal is irreversible at a temperature higher than 165°C.

4.2. Decomposition reactions

4.2.1. Nickel malonate (NiMal)

The present observations for nickel malonate decomposition (Figs. 1–4 and 9) generally confirm the results of a previous work [3] and now identify a sensitivity of reactivity to the gases present. The relatively slowest chemical change is in nitrogen where adsorbed intermediates (such as $–CH_2–CO_2–$ [3,6]) and the formation of Ni_3C are believed to diminish the participating surface area and the activity of the metal in promoting carboxylate breakdown. The presence of H_2 significantly increases the decomposition rate. The endothermic peak temperature is decreased by ca. 38°C (Fig. 4) and the exotherm associated with completion of chemical change by more than 50°C. The relatively smaller total response, composed of two overlapping peaks, shows a modification of kinetic behaviour and products, attributa-

ble to the enhanced activity of the nickel metal (Fig. 9(e)) in promoting anion breakdown.

Previous work [21] has shown that the decomposition of nickel malonate in oxygen results in conversion of all the anionic carbon to CO_2 and the residual product was NiO (studied between 250–320°C). In the present work there was evidence again that the oxygen present was capable of reacting with adsorbed carbonaceous material, thereby promoting the reactivity of the product NiO. The rate of anion breakdown was similar to that for reaction in H_2 (Fig. 2). We conclude that malonate anion breakdown in these reactions is promoted by an interface mechanism in which the solid product behaves similarly to the active phase in heterogeneous catalysis. When carbonaceous residues accumulate, in N_2 gas, or there is carbide formation, there is a decrease in decomposition rate. The reactive gases (H_2 or O_2) enhance the catalytic properties of the solid by removing surface bonded material.

4.2.2. Nickel hydrogen malonate (NiHMal)

The pattern of thermal responses for this reactant at temperatures above 300°C were closely similar to those for nickel malonate, responses occurring at ca. 8°C lower temperature (perhaps due to reactant weight loss in the first decomposition step). The residual solid reaction products from both reactions were closely similar (Figs. 9 and 10). The highly characteristic change in response peak pattern on substituting N_2 by H_2 is essentially identical with that for nickel malonate. This is a strong evidence that the same reactions occur. It is concluded that the second thermal decomposition step (above 300°C) is nickel malonate breakdown.

It is concluded from the observed pattern of response peaks (Figs. 5–7) that the intermediate reaction, 204–208°C in Fig. 5 and 214±1°C in Fig. 7, is breakdown of nickel hydrogen malonate ($C_6H_6O_8Ni$) to nickel malonate ($C_3H_2O_4Ni$). This is not unexpected and accounts for the close similarities of thermal reactions above 300°C.

References

[1] N.J. Carr, A.K. Galwey, Proc. R. Soc. London A 404 (1986) 101.
[2] A.K. Galwey, M.A. Mohamed, Solid State Ionics 42 (1990) 135.
[3] A.K. Galwey, S.G. McKee, T.R.B. Mitchell, M.A. Mohamed, M.E. Brown, A.F. Bean, Reactivity of Solids, 6 (1988) 187; see also p. 173.
[4] M.A. Mohamed, S.A. Halawy, M.M. Ebrahim, J. Anal. Appl. Pyrolysis 27 (1993) 109.
[5] M.A. Mohamed, J. Anal. Appl. Pyrolysis 30 (1994) 59.
[6] A.K. Galwey, M.A. Mohamed, J. Chem. Soc., Faraday Trans. I 81 (1985) 2503.
[7] M.A. Mohamed, J. Therm. Analysis 42 (1994) 1081.
[8] M.A. Barteau, M. Bowker, R.J. Madix, J. Catalysis 67 (1981) 118.
[9] M.A. Mohamed, S.A. Halawy, J. Therm. Analysis 41 (1994) 147.
[10] R.C. Weast (Ed.) Handbook of Chemistry and Physics, 62nd edn., CRC Press, New York, 1982.
[11] T. Ozawa, J. Thermal Anal. 7 (1975) 601.
[12] H.E. Kissinger, J. Anal. Chemistry 29 (1957) 1702.
[13] N.E. Fouad, J. Thermal Anal. 46 (1996) 1271.
[14] M.A. Mohamed, S.A.A. Mansour, M.I. Zaki, Thermochim. Acta 138 (1989) 309.
[15] K. Muraishi, K. Nagase, N. Tanaka, Thermochim. Acta 23 (1978) 125.
[16] S. Shishido, K. Ogasawara, Sci., Rep. Niigata Univ., Ser C 3 (1971) 23.
[17] K. Muraishi, K. Nagase, Thermochim. Acta 159 (1990) 225.
[18] P. Baraldi, Spectrochim. Acta, Part A 38 (1982) 51.
[19] JCPDS-ICDD, PDF2 data base (1996).
[20] T.B. Flanagan, J.W. Simons, P.M. Fichte, Chem. Commun. (1971) 370.
[21] B.R. Wheeler, A.K. Galwey, J. Chem. Soc., Faraday Trans. I 70 (1974) 661.